

## **Progress on Cherenkov Reconstruction in MICE\***

Daniel M. Kaplan,<sup>†</sup> Michael Drews, Durga Rajaram, and Miles Winter  
*Illinois Institute of Technology, Chicago, Illinois 60616, USA*

Lucien Cremaldi, David Sanders, and Don Summers  
*University of Mississippi, Oxford, Mississippi 38677, USA*

(Dated: December 10, 2015)

## Abstract

Two beamline Cherenkov detectors (Ckov-a,-b) support particle identification in the MICE beamline. Electrons and high-momentum muons and pions can be identified with good efficiency. We report on the Ckov-a,-b performance in detecting pions and muons with MICE Step I data and derive an upper limit on the pion contamination in the standard MICE muon beam.

## INTRODUCTION

The international Muon Ionization Cooling Experiment (MICE) [1] is designed to measure muon ionization cooling [2]. Cooling is needed for neutrino factories based on muon decay ( $\mu^- \rightarrow e^- \bar{\nu}_e \nu_\mu$  and  $\mu^+ \rightarrow e^+ \nu_e \bar{\nu}_\mu$ ) in storage rings [3] and for muon colliders [4].

Two high-density aerogel threshold Cherenkov counters [5], located just after the first Time of Flight counter (TOF0) in the MICE beamline, are used in support of muon and pion particle identification. The measured [6] refractive indices of the aerogels in the counters are  $n_a = 1.069 \pm 0.003$  in Ckov-a and  $n_b = 1.112 \pm 0.004$  in Ckov-b. The corresponding momentum thresholds for muons (pions) are at 280.5 (367.9) and 217.9 (285.8) MeV/c, respectively. Light is collected in each counter by four 9354KB eight-inch UV-enhanced phototubes and recorded by CAEN V1731 500 MS/s flash ADCs (FADCs).

## EVENT HANDLING AND CALIBRATION

A charge-integration algorithm identifies charge clusters  $q_i, i = 1-8$  in the FADCs where the ADC value crosses a threshold, marking times  $t_1$  and  $t_2$  at the threshold crossings, approximating the pulse beginning and end times. The time  $t_{max}$  at the cluster signal maximum is found. The charges are converted to a photoelectron count  $pe_i$ , by subtracting a pedestal  $q_{0i}$  and then normalizing by the single photoelectron charge  $q_{1i}$  for each phototube. For all  $q_i > 0$ , the total charge, arrival time,  $t_1$ , and  $t_{max}$  are stored per event.

The asymptotic  $\beta=1$  light yield  $N_{\beta=1}$  in each counter is measured using the electron peak in MICE calibration-beam runs, giving 25 and 16 photoelectrons (pe's) in Ckov-b and Ckov-a, respectively, for a nominal run. The photoelectron yields versus momentum are displayed in Fig. 1. The observed muon thresholds,  $213 \pm 4$  and  $272 \pm 3$  MeV/c, are in reasonable agreement with the expectations given above. The average number of photoelectrons for normal incidence in the counters can be predicted from the Cherenkov angle  $\cos \theta_c = 1/n\beta$ , and, near threshold  $\beta_{th} = 1/n$ ,

$$N_{pe} = N_{\beta=1} \times \sin^2 \theta_c = N_{\beta=1} \times (1 - (p_{th}/p)^2). \quad (1)$$

As seen in Fig. 2, the photoelectron spectra for  $\mu, \pi$  are observed to be Poisson-like with tails from electromagnetic showers and delta rays produced as the particle traverses TOF0 and the aerogel radiator. Secondary electrons from these processes above about 1 MeV/c produce Cherenkov light 5–6% of the time for each particle passage. For small- $N_{pe}$  signals, the measured spectra contain more zero-pe events than expected from pure Poisson-like behavior  $P_0(x) = e^{-x}$ ,  $x = \langle N_{pe} \rangle$ .

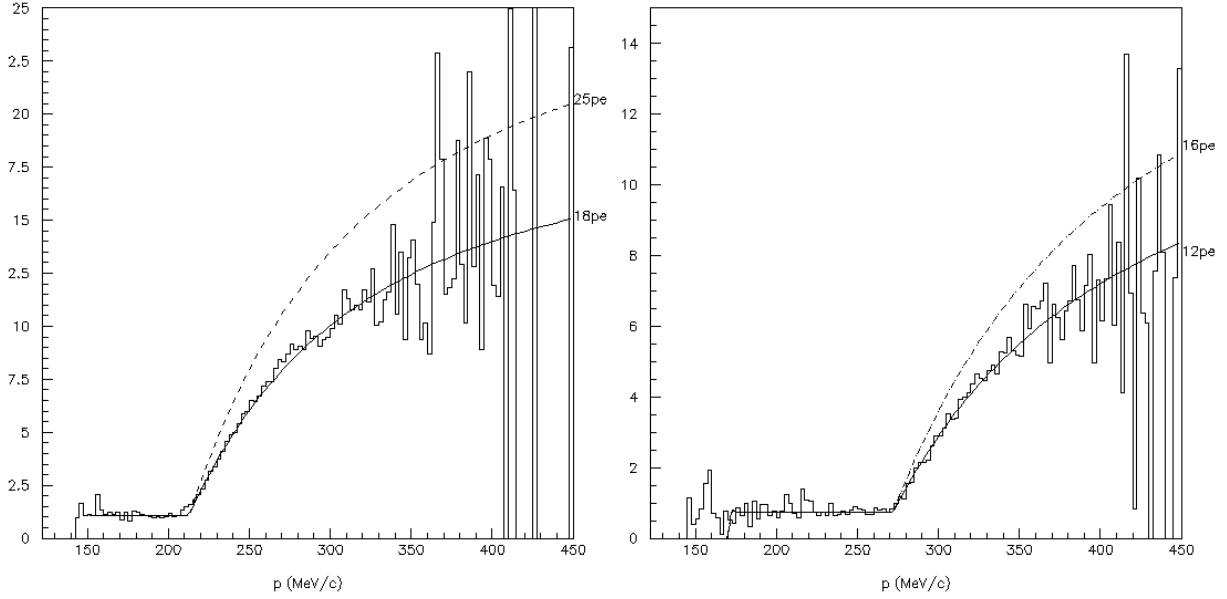


FIG. 1: Photoelectron ( $N_{pe}$ ) curves versus momentum for muons in (left) Ckov-b and (right) Ckov-a. The  $N_{\beta=1}$  values are about 75% of the values predicted from the asymptotic photoelectron spectrum of  $\beta = 1$  electrons (labeled at right)—not unexpected since for electrons TOF0 acts effectively as a “preshower” radiator.

## BEAM PARTICLE SPECTRA

The “D1” and “D2” dipoles in the MICE beamline [1] predominantly control the beam momentum and particle types transmitted into the MICE spectrometer. In the  $p_{tgt} \approx p_{D1} \approx p_{D2}$  setting (calibration mode), the beamline transports a mixture of decay/conversion electrons, decay muons, and primary pions. For  $p_{tgt} \approx p_{D1} \approx 0.5p_{D2}$ , backward muon decays from the decay solenoid (DS) are selected. G4beamline [7] Monte Carlo runs indicate that a small leakage of primary pions through the D2 selection magnet can occur at the  $\sim 1\%$  level [8]. Both these high-momentum pions and their decay muons should be observable in both Ckov-a and Ckov-b. Ckov-a can be used effectively to select the high-momentum  $\pi, \mu$  events that are just over threshold [9].

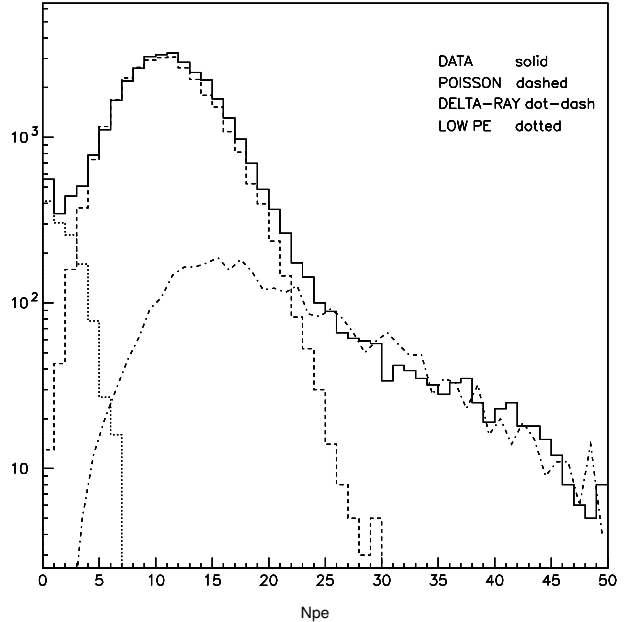


FIG. 2: Typical photoelectron spectrum seen for muons or pions above threshold in Ckov-b (solid histogram), together with model fit components: Poisson (dashed), delta-ray tail (dot-dashed), and anomalous low- $N_{pe}$  component (dotted).

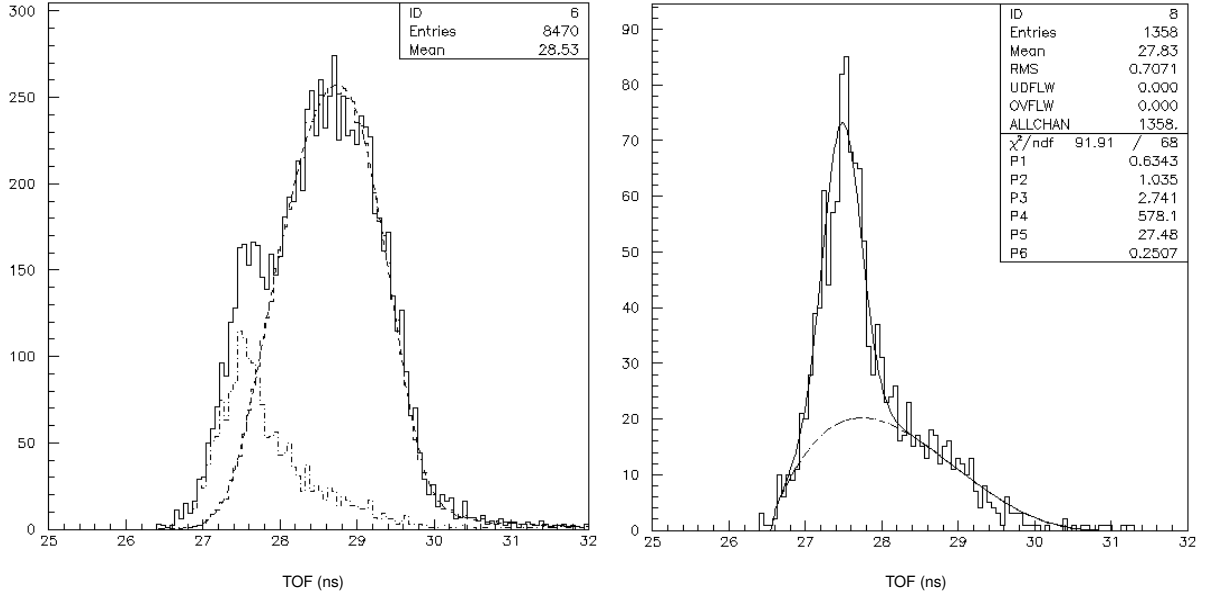


FIG. 3: Time-of-flight spectrum from TOF0 to TOF1 with (left)  $pea > 2$  cut (solid) and  $peb > 8$  cut (dot-dash), with shape of muon spectrum superimposed (dashed); and (right)  $pea > 2$  and  $peb > 10$  cuts. The  $peb$  requirements greatly reduce the delta-ray contribution. Fast  $\pi$ - $\mu$  are identified as the satellite peak centered at 27.6 ns.

## ANALYSIS

Unambiguous identification of particle species using the Cherenkov detectors (measuring velocity) would require a momentum measurement from the MICE tracker, which was not available in Step I data. Muons and pions are thus indistinguishable here by the Cherenkov effect. In the following analysis we look for high-momentum  $\pi$  or  $\mu$  that trigger Ckov-a. An additional cut on the number of photoelectrons in Ckov-b serves to suppress the  $\approx 6\%$  of slow “background” events that pass the Ckov-a cut due to delta-ray emission.

We analyzed 120k Step I muon events with  $p_{tgt} = 400$  MeV/ $c$  and  $p_{D2} = 237$  MeV/ $c$  (the “standard” muon beam settings). We also analyzed 35k muon events with  $p_{tgt} = 500$  MeV/ $c$  and  $p_{D2} = 294$  MeV/ $c$ . In Fig. 3 we cut away the electron signal (by requiring  $tof > 26.4$  ns) and also make a Ckov-a  $N_{pe} > 2$  cut. The shoulder centered at 27.6 ns is made up of fast muons and pions triggering in Ckov-a and at TOF1. The background events centered approximately at  $tof = 28$  ns are from particles with momenta below threshold in Ckov-a, but giving  $N_{pe} > 2$  Ckov-a light by delta-ray emission. This background is consistent with the expected 6% contamination level. The  $tof = 27.6$  ns peak corresponds to  $p_{\mu} = 277$  MeV/ $c$  or  $p_{\pi} = 363$  MeV/ $c$ , both above threshold in Ckov-a.

Fast muons and pions will leave considerable light in Ckov-b. According to Eq. 1 about 10 pe will be produced in Ckov-b at  $p_{\mu} = 270$  MeV/ $c$ . The probability for simultaneous delta-ray detection in *both* Ckov-a *and* Ckov-b will be about  $0.06^2 = 3.6 \times 10^{-3}$ . In Fig. 3 (right) we add a Ckov-b  $N_{pe} > 10$  cut. The delta-ray background is substantially reduced

to about 500 events. A fit to Gaussian signal and phase-space background of the form ( $x \equiv$  time of flight)  $f = N(\sqrt{2\pi}\sigma)^{-1}e^{-(x-x_0)^2/2\sigma^2} + B(x-x_{lo})^\alpha(x_{hi}-x)^\beta$  gives  $539 \pm 34$  signal events. When corrected for efficiency [9] we obtain  $N = 1002 \pm 56$  events. By varying the fitting parameters we find a  $\pm 101$ -event systematic (syst) uncertainty [9]. The fast  $\pi$ - $\mu$  fraction is thus  $R_{\mu\pi} = (1002 \pm 56 \pm 101)/118,793 = [0.84 \pm 0.05$  (stat)  $\pm 0.09$  (syst)]%.

If we assume pessimistically that all fast  $\pi$ - $\mu$  are pions, we can obtain upper limits on the pion fraction:  $R_{\mu\pi} < 0.97\%$  (90% CL) and  $R_{\mu\pi} < 1.00\%$  (95% CL). Any Bayesian model would require some prior knowledge of the pion-to-muon ratio in the beam. Estimating this (based on the G4beamline simulation) to be about 1/20 (or about 50 pions) allows us to estimate the fraction of pions in the beam to be  $\pi/\mu \simeq 50/119,000 = 0.04\%$ —indeed very small, surpassing the MICE design requirements.

---

\* Presented at NuFact15, 10-15 Aug 2015, Rio de Janeiro, Brazil [C15-08-10.2]; work supported by U.S. DOE via the MAP Collaboration.

† Electronic address: [kaplan@iit.edu](mailto:kaplan@iit.edu); presenter

- [1] M. Bogomilov *et al.*, JINST **7** (2012) P05009; D. Adams *et al.*, Eur. Phys. J. **C73** (2013) 2582; D. Adams *et al.*, arXiv:1510.08306; M. Bogomilov *et al.*, arXiv:1511.00556.
- [2] D. Neuffer, arXiv:1312.1266; D. Neuffer, AIP Conf. Proc. **441** (1998) 270; R. B. Palmer *et al.*, Phys. Rev. ST Accel. Beams **8** (2005) 061003; P. Snopok *et al.*, Int. J. Mod. Phys. **A24** (2009) 987; J. C. Gallardo and M. S. Zisman, AIP Conf Proc. **1222** (2010) 308; M. Chung *et al.*, Phys. Rev. Lett. **111** (2013) 184802; C. Yoshikawa *et al.*, IPAC-2014-TUPME016; D. Stratakis and R. B. Palmer, Phys. Rev. ST Accel. Beams **18** (2015) 031003; J. G. Acosta *et al.*, COOL-2015-MOPF07.
- [3] D. G. Koshkarev, CERN-ISR-DI-74-62 (1974); D. Cline and D. Neuffer, AIP Conf. Proc. **68** (1980) 856; D. Neuffer, IEEE Trans. Nucl. Sci. **28** (1981) 2034; S. Ozaki, R. B. Palmer, M. S. Zisman *et al.*, BNL-52623 (2001); M. M. Alsharo'a *et al.*, Phys. Rev. ST Accel. Beams **6** (2003) 081001; S. Choubey *et al.*, arXiv:1112.2853; D. Adey *et al.*, Phys. Rev. **D80** (2014) 071301.
- [4] C. M. Ankenbrandt *et al.*, Phys. Rev. ST Accel. Beams **2** (1998) 081001; J. G. Gallardo *et al.*, Snowmass 1996, BNL-52503; R. B. Palmer *et al.*, Nucl. Phys. Proc. Suppl. **51A** (1996) 61; D. Neuffer and R. Palmer, Conf. Proc. C940627 (1995) 52; A. V. Tollestrup, Conf. Proc. C9610311 (1996) 221; A. M. Sessler, Phys. Today **51N3** (1998) 48.
- [5] L. Cremaldi *et al.*, IEEE Trans. Nucl. Sci. **56** (2009) 1475; D. A. Sanders, Conf. Proc. C090504 (2009) 1696.
- [6] L. Cremaldi *et al.*, “Examination of Matsushita High Density Aerogel,” MICE-NOTE-149, Sept. 2006, <http://mice.iit.edu/micenotes/public/pdf/MICE0149/MICE0149.pdf>.
- [7] T. J. Roberts *et al.*, Conf. Proc. C0806233 (2008) WEPP120.
- [8] Pions leaking through D2 produce high-momentum decay muons in the MICE beam—a different production mechanism than that of the nominal MICE beam, which comes from pion decays *upstream* of D2.
- [9] More details of the analysis may be found in L. Cremaldi *et al.*, MICE Note 473 (2015), <http://mice.iit.edu/micenotes/public/pdf/MICE0473/MICE0473.pdf>.